EXPERIMENTAL AND THEORETICAL INVESTIGATIONS OF 2-D VACUUM POWER FLOW

S.B. Swanekamp[a)], J.M. Grossmann, D.D. Hinshelwood[a)],
S.J. Stephanakis, J.R. Boller, and R.J. Commisso
Plasma Physics Division
Naval Research Laboratory
Washington, DC 20375

Simulations of vacuum electron flow in a coaxial transmission line with and without ion emission are compared with each other and with experimental data from Gamble II. The simulation without ions shows large current losses just downstream of an impedance discontinuity. Simulations with ions show that the vacuum electron current past the impedance discontinuity is increased by the presence of ions. The losses are much more distributed than in the simulation without ions. The experimental data shows a more distributed current loss that is similar to the case where ion emission is allowed. This suggests that ions may be present and playing a role in the experiment.

With the trend towards multi-modular high power systems, understanding power flow through complicated two and three dimensional (2-D and 3-D) structures is vital to realizing the full potential of many advanced pulsed-power designs. Some examples of complex 3-D structures used in advanced multi-modular systems include convolutes and transitions between coaxial and triplate transmission lines. One of the main tools for analyzing power-flow in such structures is the particle-in-cell (PIC) code. Before these tools can be used with confidence it is necessary to benchmark these codes with experiments in simple geometries that are very well diagnosed. This paper presents comparisons between 2-D PIC simulations with experimental measurements made on the Gamble II accelerator. The simulations are performed with and without ion emission from the anode. The simulation without ions shows very localized current losses whereas simulations with ion emission from the anode show more distributed current losses and is in better agreement with experimental data.

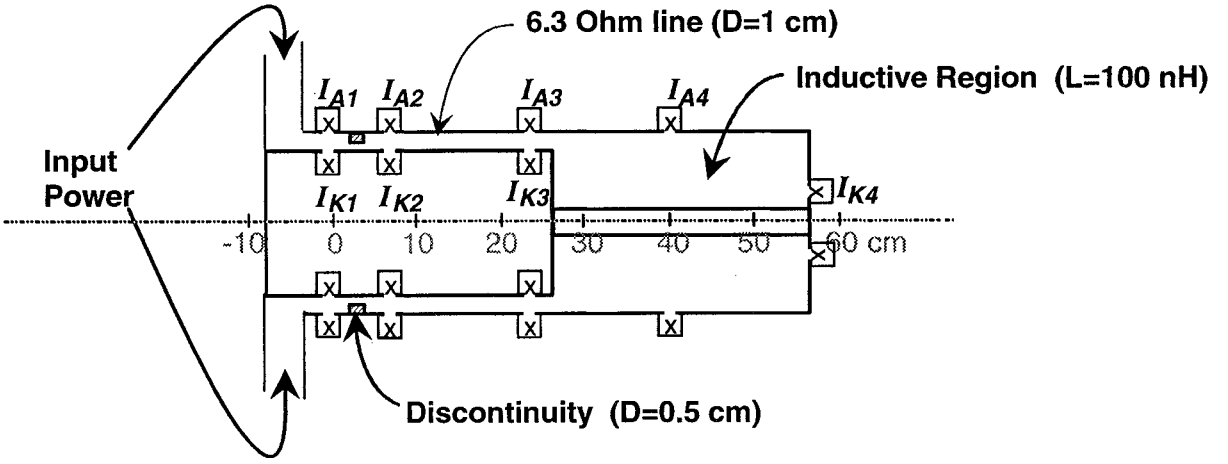

Figure 1. Schematic of the Gamble II power-flow hardware.

A schematic of the power-flow hardware fielded on the front end of Gamble II is shown in Fig. 1. A 6.3 Ω coaxial transmission line with a 1 cm anode-cathode (A-K) gap is terminated by a

Report Documentation Page

Form Approved
OMB No. 0704-0188

1. REPORT DATE	2. REPORT TYPE	3. DATES COVERED
JUL 1995	**N/A**	**-**

4. TITLE AND SUBTITLE	5a. CONTRACT NUMBER
Experimental And Theoretical Investigations Of 2-D Vacuum Power Flow	5b. GRANT NUMBER
	5c. PROGRAM ELEMENT NUMBER
6. AUTHOR(S)	5d. PROJECT NUMBER
	5e. TASK NUMBER
	5f. WORK UNIT NUMBER
7. PERFORMING ORGANIZATION NAME(S) AND ADDRESS(ES) **Plasma Physics Division Naval Research Laboratory Washington, DC 20375**	8. PERFORMING ORGANIZATION REPORT NUMBER
9. SPONSORING/MONITORING AGENCY NAME(S) AND ADDRESS(ES)	10. SPONSOR/MONITOR'S ACRONYM(S)
	11. SPONSOR/MONITOR'S REPORT NUMBER(S)

12. DISTRIBUTION/AVAILABILITY STATEMENT
Approved for public release, distribution unlimited

13. SUPPLEMENTARY NOTES
See also ADM002371. 2013 IEEE Pulsed Power Conference, Digest of Technical Papers 1976-2013, and Abstracts of the 2013 IEEE International Conference on Plasma Science. Held in San Francisco, CA on 16-21 June 2013. U.S. Government or Federal Purpose Rights License.

14. ABSTRACT

15. SUBJECT TERMS

16. SECURITY CLASSIFICATION OF:			17. LIMITATION OF ABSTRACT	18. NUMBER OF PAGES	19a. NAME OF RESPONSIBLE PERSON
a. REPORT **unclassified**	b. ABSTRACT **unclassified**	c. THIS PAGE **unclassified**	**SAR**	**6**	

highly inductive section. This high inductance section acts as a high impedance load early in time and gradually becomes a low impedance load late in time as the current derivative approaches zero. Vacuum electron flow is launched into the 6.3 Ω transmission line at a localized impedance discontinuity where the local gap size is decreased from 1 cm to 0.5 cm. The vacuum electron flow downstream of the impedance discontinuity is diagnosed by a series of anode and cathode B-dot current probes (I_{A1-4} and I_{K1-4}).

A computational model of the geometry depicted in Fig. 1 was setup in the 2-D PIC code MAGIC[1]. A simplified one dimensional transmission line model of the Gamble II accelerator consisting of an open circuit voltage (3 MV, 85 ns FWHM) and an equivalent generator resistance of 2 Ω was used to drive a TEM wave into the 2-D simulation. In all the simulations described in this paper, the entire cathode surface was treated as a space-charge-limited electron emitter. Simulations results are presented with and without space-charge-limited proton emission from the anode in the 6.3 Ω line downstream of the impedance discontinuity. Ion emission in the inductive region was not allowed in either of the simulations.

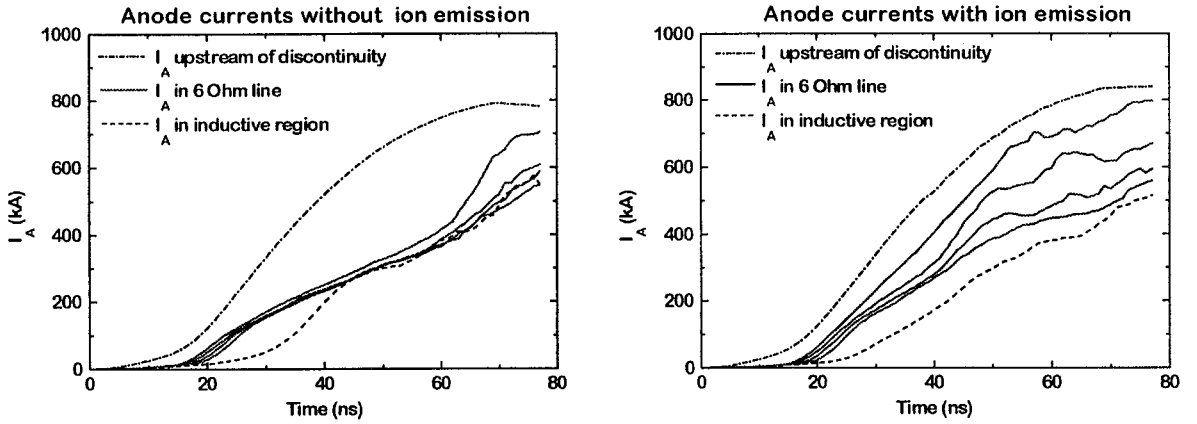

(a) (b)

Fig. 2. The calculated anode currents (a) for the simulation without ions and (b) with proton emission in the 6.3 Ω line. The dashed curves are calculated anode currents in the inductive section.

Figure 2 shows the anode currents at 5 cm intervals starting just upstream of the impedance discontinuity (z=0). The anode currents for the simulation without ions, shown in Fig. 2a, indicate large current losses just downstream of the impedance discontinuity and very little current losses elsewhere in the 6.3 Ω line. The electron loss just downstream of the impedance discontinuity carries a sufficient amount of energy to the anode (hundreds of J/gm) to create an anode plasma.[2] Figure 2a also shows that some current is lost at the transition between the 6.3 Ω line and the inductive load for t<40 ns. The anode currents for the simulation with proton emission, shown in Fig. 2b, indicate less current loss associated with the impedance discontinuity. From Fig. 2b it is also seen that, when ions are present, the current losses are distributed throughout the 6.3 Ω line. Figure 2b further shows that current losses at the transition between the 6.3 Ω line and the inductive load are present over a longer time scale for the simulation with ions. This current loss is from both electrons and ions. Although ion and electron currents were not distinguished in the simulation,

estimates from the Child-Langmuir[3] (C-L) law predict that, at a peak voltage of 1.2 MV, the ion current is 75 kA for the present geometry. This is a lower bound for the ion current since magnetically insulated electron flow can enhance the ion current over the C-L value.

One possible explanation for the increased vacuum electron current in the 6.3 Ω line when proton emission is allowed is that the region downstream of the impedance discontinuity behaves similarly to a pinched beam diode.[4] If ion emission does not occur a large fraction of the electron flow strikes the anode about one Larmor radius downstream of the impedance discontinuity. When the electrons deposit enough energy to the anode an anode plasma forms that reduces the anode electric field and provides a space-charge-limited source of ions.[2] The reduced anode electric field allows the magnetic force to prevent the electrons which enter the anode plasma from striking the anode surface. These electrons move axially down the transmission line and strike the anode in a new region where, if enough energy is deposited, plasma forms on a new portion of the anode and electron flow propagates down the transmission line. For simplicity, ion emission in MAGIC is enabled after a specified electric field exists on the anode surface (100 kV/cm) and not turned on by electron beam energy deposition to the surface. Therefore, the simulations with ion emission do not adequately model the detailed process of anode plasma formation but provide insight to the effects of ions in magnetically insulated flows.

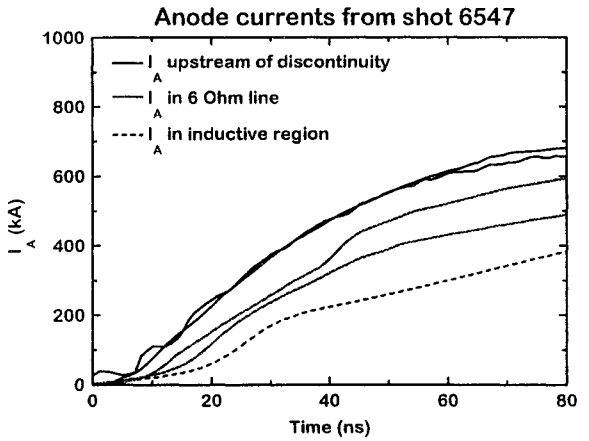

Fig. 3. The measured anode currents in the Gamble II experiment. The dashed curve is in the inductive section.

The anode currents measured on Gamble II are shown in Fig. (3). The measurements show a distributed electron loss in the 6.3 Ω line. These results are similar to the simulation results with ion emission enabled. This suggests that ions are present in the Gamble II experiment. However, because plasma can magnetically shield the B-dots, there is a reasonably large uncertainty associated with these measurements. Additional experiments are necessary to provide better current measurements and more clearly determine the role of ions. Notice that the peak current in the Gamble II shot is slightly lower than the peak current in the simulation. This difference is due to a slightly higher open circuit voltage used in the simulation than what was produced during the shot.

Current enclosed contours (50 kA between contours) at t=50 ns for (a) the simulation without ions and (b) the simulation with ion emission in the 6.3 Ω line are shown in Figure 4. At this time

there is about 650 kA upstream of the impedance discontinuity and the cathode current downstream of the impedance discontinuity is approximately 200 kA for both cases. The simulation without ions shows about 300 kA is lost just downstream of the impedance discontinuity. Approximately 150 kA flows in the vacuum with relatively little current loss in the 6.3 Ω line. By contrast, the simulation with ion emission has only about 50 kA of loss current at the impedance discontinuity and nearly 200 kA of distributed current loss in the 6.3 Ω line. In addition Fig. 4b shows that the additional vacuum electron current flows primarily near the anode. This might be expected since this is where most of the ion space charge resides. The propagation of vacuum electron current with ions produced on the anode may also occur during the power transfer phase of the plasma-opening switch.

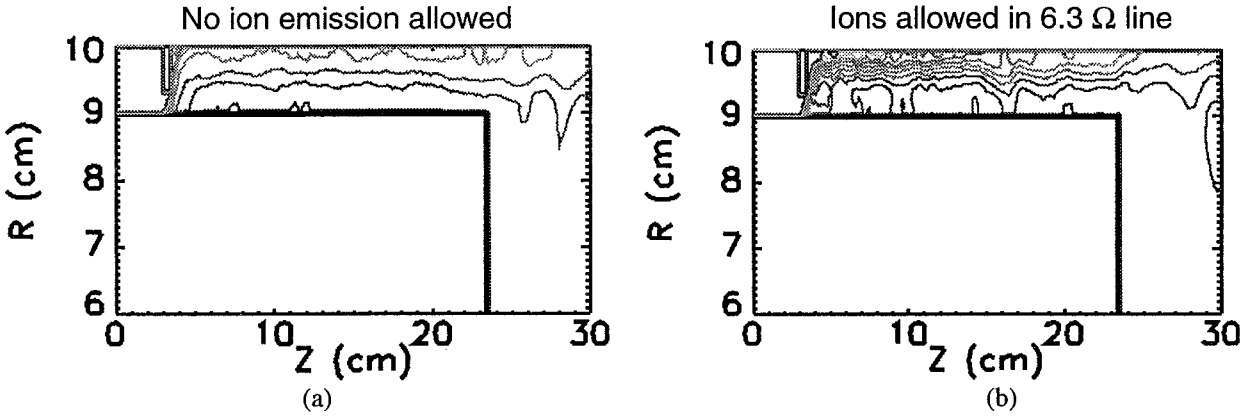

Fig. 4. Current enclosed contours at t=50 ns for (a) the simulation without ions and (b) the case with proton emission in the 6.3 Ω line.

Vacuum electron flow in the 6.3 Ω line can be analyzed using the flow impedance concept. If the electrons are E×B drifting and there are no ions in the line, then pressure is balanced across the electron flow and the flow impedance can be written as[5]

$$Z_f = \frac{V}{\left(I_A^2 - I_C^2\right)^{1/2}} \quad , \tag{1}$$

where V is the voltage, I_A is the local anode current and I_C is the local cathode current. For a localized impedance discontinuity it is customary to use the anode current just upstream of the discontinuity and the cathode current just downstream of the discontinuity. An idealized electron flow pattern is shown in Fig. 5. A physical interpretation of the flow impedance can be described as follows. If the anode-cathode gap spacing, D, of a coaxial transmission line is small compared to the cathode radius, R_C, then it can be shown that Eq. (1) is equivalent to the vacuum wave impedance between the centroid of the electron space charge ($\bar{x}$) and the anode ($Z_f=60\,(D-\bar{x})/R_C$).[6] The size of the electron sheath can be estimated from the electron Larmor radius which, in turn, can be estimated from the critical current formula and expressed as

$$D_{CRIT}[\,cm\,] = 8500 F_{CR} \frac{R_C[\,cm\,]}{I_A[\,A\,]} (\gamma^2 - 1)^{1/2} \tag{2}$$

In Eq. (2) γ is the relativistic mass factor and F_{CR} is a factor that is weakly dependent on voltage and approximately 1.6 for voltages between 1 and 3 MV.[7] If it is assumed that the electron charge is evenly distributed in the electron sheath, then the charge centroid is approximately $D_{crit}/2$ and the flow impedance can be written as

$$Z_f \cong 60(D-D_{crit}/2)/R_c \ . \qquad (3)$$

When the vacuum electrons are very well insulated then D_{crit} is very close zero and the flow impedance is the vacuum wave impedance of the transmission line, $Z_f \cong 60D/R_C$. When the electron flow is critically insulated (i.e. the electron gyroradius is comparable to the anode-cathode spacing of the transmission line) then $D_{crit}=D$ and the flow impedance is half the vacuum wave impedance of the transmission line, $Z_f \cong 30D/R_C$. It is important to note that, when ions are present and unmagnetized, the flow impedance defined by Eq. (1) no longer applies since the presence of ions alters the pressure balance relation.

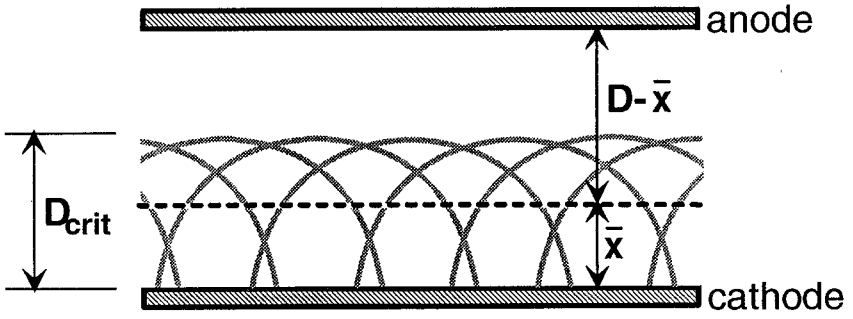

Fig. 5. An idealized electron flow pattern and the relationship between the D_{crit}, $\bar{x}$, and D.

The critical gap size and the flow impedance calculated with the voltages and currents from the simulation without ions are shown in Figs. 6a and 6b. The physical gap size and half the vacuum wave impedance for both the impedance discontinuity and the 6.3 Ω line are also shown by dashed lines in the two figures. Figure 6a shows that D_{crit} is approximately equal to 0.5 cm in the impedance discontinuity and 1.0 cm in the 6.3 Ω line indicating that the electron flow is critically insulated over most of the simulation. Therefore, for the simulation without ions, the system sheds precisely enough current near the impedance discontinuity to keep the electron flow critically insulated. The flow impedance is also close to half the vacuum wave impedance over most of the simulation. This is consistent with the conclusion that the electron flow is critically insulated. Late in time, as the inductive load begins to look more like a short circuit, the electron Larmor radius gets smaller. When this happens Eq. (3) predicts that the flow impedance should get larger and approach the vacuum wave impedance of the line. This happens at z=20 cm but does not occur at z=5 cm. The electron density contours late in time indicate that the electron charge at z=5 cm is not evenly distributed in the sheath but more concentrated near the anode. This causes the flow impedance at z=5 cm to decrease late in time even though the Larmor radius is decreasing.

The critical gap size calculated with the voltages and currents from the simulation with proton emission in the 6.3 Ω line is shown in Fig. 7. Figure 7 shows that the electron Larmor radius with

ions is significantly smaller than the no ion case. This is due primarily to an increase in the anode current in the 6.3 Ω line when ions are present.

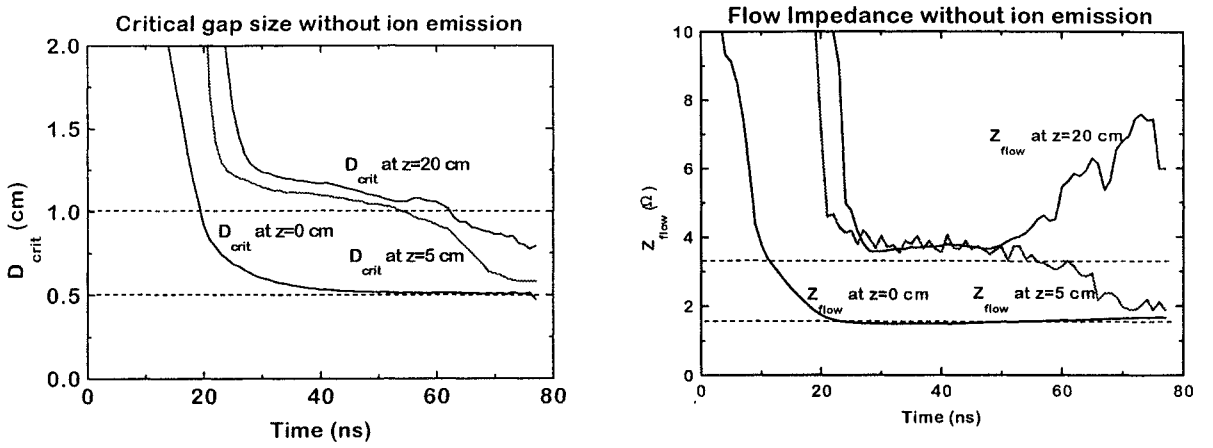

(a) (b)

Fig. 6. (a) The critical gap size and (b) the flow impedance at several positions in the 6.3 Ω line without ions.

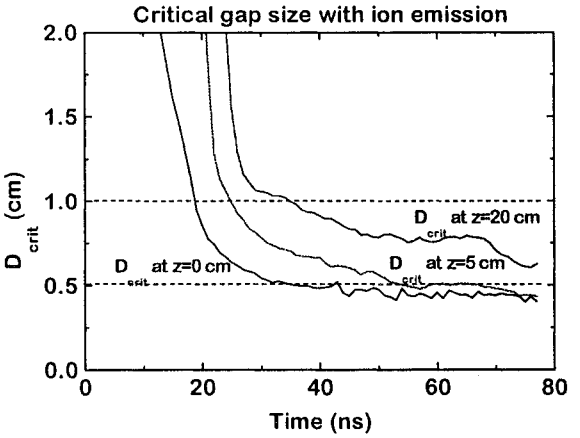

Fig. 7. The critical gap size at several positions in the 6.3 Ω line with proton emission from the anode.

The authors would like the thank P.F. Ottinger, G. Cooperstein, D. Mosher, Jess Neri and the rest of the Pulsed Power Physics Branch of the Naval Research Laboratory for their interest in this work.

a) JAYCOR, Vienna, VA 22182.

Work supported by DNA.

---

[1] B. Goplen, L. Ludeking, D. Smithe, and G. Warren, Computer Physics Communications 87 (1994), 54.
[2] A. Blaugrund, G. Cooperstein, and S.A. Goldstein, Phys. Fluids 20, 1185 (1977).
[3] C.L. Child, Phys. Rev. **32**, 492 (1928). I. Langmuir, Phys. Rev. 33, 954 (1929).
[4] R.B. Miller, *An Introduction to the Physics of Intense Charged Particle Beams*, Plenum Press, New York, pp. 67-70 (1982).
[5] C.L. Mendel, Jr., M.E. Savage, D.M. Zagar, W.W. Simpson, J.W. Grasser, and J.P. Quintenz, J. Appl. Phys. 71, 3731 (1992).
[6] C.L. Mendel, private communication.
[7] R.J. Barker and S.A. Goldstein, Bull. Am. Phys. Soc. 26, 921 (1981).